

The Study of Fluidized Beds of Class A and B Particles Using Electrical Capacitance Volume Tomography

Chris Zuccarelli¹, Benjamin Straiton¹, Joshua Sines¹, Qussai Marashdeh¹

¹Tech4Imaging, 1910 Crown Park Court, Columbus, Ohio, 43235, USA

ABSTRACT: Electrical Capacitance Volume Tomography (ECVT) is a real-time 3D imaging and measurement technique for the online study of multiphase flow behavior. Here, it is applied for the study of two fluidized beds, one with Geldart Class A particles and another with Class B particles. A straight cylindrical column was constructed and an experiment conducted where the air mass flow rate through the column was varied. An ECVT system was used to capture real-time, three-dimensional data about the fluidized beds, and this data was analyzed to determine important factors about the fluidized beds, such as void fraction, bubble size, bubble frequency, and bubble velocity.

Keywords: Fluidized Bed, Fluidized Bed Reactor, Circulating Fluidized Bed, FCC Riser Reactor, Pneumatic Conveying, Drying and Mixing, Flow Monitoring, Bubble Column, Agglomeration, Solid Separation, Phase Separation, Segregation, Phase Reaction, Solids Holdup, Volume Fraction, Void Fraction, Phase Distribution, Velocimetry, Bubble Size, Bubble Velocity, Bubble Frequency, Electrical Capacitance Volume Tomography, Electrical Capacitance Tomography

I. Introduction

In many chemical and power generation applications, the proper fluidization of solid particles is optimal for solid-gas contact and reaction. Fluidized bed reactors are affected by fluidization characteristics such as bubble frequency, size, and velocity. It is important to measure and study such characteristics and adjust reactor settings to optimize these parameters. This information can lead to improved design, scale-up, and performance of fluidized beds, and lead to accurate performance predictions of multiphase flow systems.

Numerous technologies have been applied for the in-situ measurement and study of fluidized beds. Probes, whether thermal, optical, pressure or otherwise, are intrusive and provide only localized measurements. Non-intrusive measurement techniques such as magnetic resonance imaging, nuclear resonance, and laser-Doppler velocimetry (LDV) can be

impractical and hazardous. Computational Particle Fluid Dynamics (CPFD) simulations provide insight into the behavior of fluidized beds, but do not provide true measurements. A more practical method of flow validation is desired for the online monitoring of these beds. Electrical Capacitance Volume Tomography (ECVT) is a noninvasive, real-time imaging and measurement method that can be used for the study of gas-solid beds and reactor columns.

II. Theory

Professor Derek Geldart, through the careful observation of the fluidization of many types of particles, created a classification system for solids based on particle behavior. Class A particles fluidize easily, with small, controlled bubbling. Class B particles also fluidize well, with bubbles that grow in size and behave more erratically. Class C particles are very fine, and do not fluidize easily due to interparticle forces. Class D particles are large and dense, making them also difficult to fluidize. When fluidized,

Class D particles create large, explosive bubbles or spouting channels. This classification system is quite useful for the organization of solids and their fluidization behaviors [1].

ECVT is a natural extension of Electrical Capacitance Tomography that collects noninvasive capacitance measurements on a 3D space. An ECVT system consists of three major components: a passive sensor comprised of plate electrodes which surround a region to be studied, a data acquisition system that sends and receives electric field data from the sensor, and software to interface with the acquisition system and interpret its data in real time. Figure 1 shows a diagram of these three components.

With this ECVT system, distributions of electric field are measured with the multitude of electrodes on the sensor. The measured fields are related to the dielectric constant distribution within the sensing region via proprietary algorithms within the Tech4Imaging software [2]. Tech4Imaging's ECVT system has been proven for the noninvasive analysis of gas-solid systems [3], and has been compared with MRI techniques for the same purpose [3, 4]. Given the scalability and noninvasive nature of ECVT, this measurement technique can be applied to numerous multiphase flow scenarios. Here, an ECVT system is used to analyze the two-phase flow of gas and solids in fluidized beds of Class A and B particles.



Figure 1: The three major components of an ECVT system (from left to right): a sensor surrounding the flow, a data acquisition system, and data analysis software.

III. Experimental Setup

The Geldart Class A particle used was aluminum oxide grit with a mesh range of 230-325, which translates to a particle diameter range of 44 to 63 microns.

The Geldart Class B particle used was dry play sand, with a particle diameter range of 1/8 mm to ¼ mm.

The column used was an acrylic tube with an outer diameter of 2.5 inches (6.35 cm), an inner diameter of 2.375 inches (6.0325 cm), and a length of 2 feet (60.96 cm). A rubber stopper was placed on one end of the tube, with a 1/8 inch (0.3175 cm) diameter hole in the center of the stopper. A one-way check valve was inserted into the hole. This valve was connected to an air compressor. The compressor was used to control the volumetric flow rate of air into the bed of solids. The air flow rate was adjusted from a range of 0 to 50 standard cubic feet per hour (0 to 1416 liters per hour, or LPH).

The ECVT sensor used was 3D printed from ABS plastic and fabricated with conductive nickel paint and female BNC ports. The sensor had an inner diameter of 2.5 inches (6.35 cm), and a height of 4.25 inches (10.795 cm). The ECVT sensor consisted of 24 plate-shaped electrodes, in four axial layers of 6 plates each. This sensor was attached to the exterior of the acrylic tube, with the sensor's bottom end 4 inches (10.16 cm) above the rubber stopper at the end of the acrylic tube. Figures 2 and 3 show a diagram and photo of the setup, respectively.

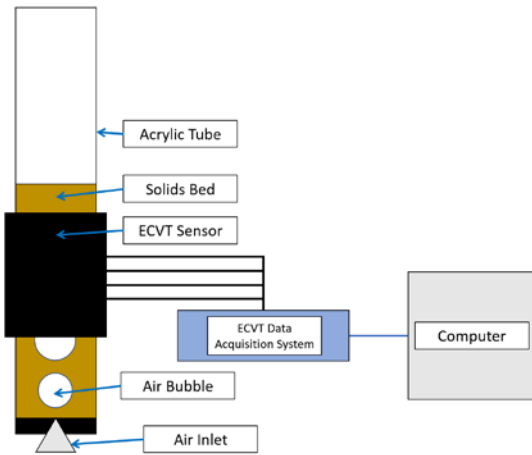


Figure 2: Setup of Fluidized Bed Experiment

The sensor was connected with coaxial cables to Tech4Imaging’s patented Electrical Capacitance Volume Tomography system. This system was used to collect real-time data about the fluidized beds. The system sequentially excites the sensor plates with an AC voltage and receives capacitance readings from the other plates. The plates were excited with a 250-kilohertz wave at a 5 V peak amplitude. The system collected an average of 40 measurements a second. The excitation frequency, voltage, and data acquisition speed were all selected based on the particles being studied. The Tech4Imaging ECVT system operating conditions are adjustable to fit into a wide variety of measurement scenarios.

The ECVT system was connected to a PC with a USB 2.0 cable connection, and the system was controlled with Tech4Imaging’s 4Sight software. This software was used to interface and operate the ECVT system, as well as analyze the capacitance data in real-time and in post-processing.



Figure 3: Picture of ECVT sensor around sand fluidized bed column. A rising air bubble can be seen at the 10.5 inch mark.

The acrylic tube was filled with sand to a bed height of 11 inches (27.94 cm), with the top of the bed rising about 2 inches (5.08 cm) above the top of the ECVT sensor. The air flow rate was raised from 0 to 20 standard cubic feet per hour (0 to 566.4 liters per hour) to begin the sand fluidization. Then, the air flow rate was set to 20, 25, 30, 40 and 50 SCFH (566.4, 708, 849.6, 1132.8, and 1416 LPH) and capacitance data was captured at each of these steady fluidization states for 5 seconds (or 200 measurements captured at 40 measurements per second).

This experiment was repeated with the aluminum oxide bed, with a static bed height of 10.50 inches (26.67 cm). However, the air flow rate only needed to be raised to 10 SCFH (283.2 LPH) to begin fluidization. Then, capacitance data was captured at steady fluidization states with the air flow rate set to 10, 20, 30, 40 and

50 SCFH (283.2, 566.4, 849.6, 1132.8, and 1416 LPH).

The experiments were conducted at standard temperature and pressure.

IV. Experimental Results

Several metrics about the fluidized beds were extracted from the Tech4Imaging ECVT system and software. Metrics about average solids volume fraction, void fraction, bubble size, bubble speed, and bubble frequency were measured. A summary of these metrics is presented in Table 1 and Table 2.

Table 1: Metrics for Class A Particle Fluidized Bed

Class A Particle (Aluminum Oxide) Bed				
Air Flow Rate, SCFH, [LPH]	Average Void Fraction	Average Bubble Radius, in, [cm]	Average Bubble Velocity in/sec, [cm/sec]	Average Bubble Frequency (Hz)
0	0.360	0	0	0
10 [283.2]	0.470	0.79 [2.01]	13.91 [35.33]	3.2
20 [566.4]	0.560	0.92 [2.34]	15.24 [38.71]	3.6
30 [849.6]	0.620	1.01 [2.57]	17.78 [45.16]	4.0
40 [1132.8]	0.640	1.02 [2.59]	20.00 [50.8]	4.0
50 [1416]	0.680	1.06 [2.69]	22.85 [58.04]	4.2

Table 2: Metrics for Class B Particle Fluidized Bed

Class B Particle (Sand) Bed				
Air Flow Rate SCFH, [LPH]	Average Void Fraction	Average Bubble Radius, in, [cm]	Average Bubble Velocity in/sec, [cm/sec]	Average Bubble Frequency (Hz)
0	0.360	0	0	0
20 [566.4]	0.380	0.39 [0.99]	8.89 [22.58]	1.4
25 [708]	0.390	0.60 [1.52]	13.33 [33.86]	1.4
30 [849.6]	0.410	0.66 [1.68]	14.81 [37.62]	1.6
40 [1132.8]	0.470	0.86 [2.18]	16.67 [42.34]	2
50 [1416]	0.610	0.92 [2.34]	21.05 [53.47]	2.8

To determine solids volume fraction and void fraction, the ECVT measurements were averaged together. The system was calibrated against a static bed of the solids at its highest packing ratio, which was 0.64. The solids fraction is the average of the ECVT measurements, and the void fraction is the difference between 1 and the solids fraction. This method was used to generate the second column of Tables 1 and 2.

$$\text{Void Fraction} = 1 - \text{Solids Fraction} \quad (1)$$

As measurements were being taken with the ECVT system, the fluidized bed was filmed with a high-definition camera. The film was used to observe the solid bed height fluctuation at each flow rate. From the observed bed height, the solids fraction and void fraction in the fluidized bed could be found with Equations (1) and (2):

$$\text{Solids Fraction} = \frac{\text{Static Solids Bed Height}}{\text{Fluidized Bed Height}} * 0.64 \quad (2)$$

This method of measuring void fraction is prone to some errors. The solids surface of a fluidized bed is constantly fluctuating, and visually measuring the surface level has its own amount of error.

Furthermore, this method of determining void fraction only determines the total void fraction of the entire fluidized bed and it is assumed that this is representative of the average void fraction in the ECVT sensing region. Tables 3 and 4 show the visual estimation of bed void fraction, compared with the void fraction as measured by the ECVT system.

It can be seen that the error between the visual estimation and ECVT measurement of void fraction increases with air flow rate. The reason for this is because the visual estimation of void fraction becomes much less accurate for higher air flow rates, as the bed surface becomes more turbulent and more difficult to measure, as well as the fact that measuring the bed height does not give any indication of the solids distribution, or packing ratio, within the fluidized bed. The visually-estimated bed height may be very inaccurate for turbulent flow. Thus, the visual and ECVT void fractions were less similar for violent fluidizations.

Table 3: Void Fraction of Class A Particle Fluidized Bed

Class A Particle (Aluminum Oxide) Bed			
Air Flow Rate, SCFH, [LPH]	Average Bed Height, in, [cm]	Average Void Fraction (Visual)	Average Void Fraction (ECVT)
0	10.50 [26.67]	0.360	0.360
10 [283.2]	12.00 [30.48]	0.440	0.470
20 [566.4]	13.00 [33.02]	0.480	0.560
30 [849.6]	13.50 [34.29]	0.500	0.620
40 [1132.8]	14.00 [35.56]	0.520	0.640
50 [1416]	14.25 [36.20]	0.530	0.680

Table 4: Void Fraction of Class B Particle Fluidized Bed

Class B Particle (Sand) Bed			
Air Flow Rate SCFH, [LPH]	Average Bed Height, in, [cm]	Average Void Fraction (Visual)	Average Void Fraction (ECVT)
0	11.00 [27.94]	0.360	0.360
20 [566.4]	11.05 [28.07]	0.363	0.380
25 [708]	11.25 [28.56]	0.375	0.390
30 [849.6]	11.50 [29.21]	0.388	0.410
40 [1132.8]	12.00 [30.48]	0.413	0.470
50 [1416]	12.50 [31.75]	0.437	0.610

Figures 4 and 7 show plots of the real-time solids volume fraction of the fluidized beds over the 5 second measurement period. It can be seen that the solids fraction pulses periodically as bubbles move up through the fluidized bed.

It can be inferred that a bubble is passing through the ECVT sensing region when the solids fraction reaches a local minimum. The bubble frequency was determined by taking the average time difference between the appearances of bubbles in the ECVT sensing region. This method was used to generate the fifth column of Tables 1 and 2.

Along with real-time solids fraction and void fraction, the time-averaged solids fraction as a function of space was analyzed with the Tech4Imaging ECVT system and software. This was done by averaging together all the measurements made over the 5 second capture time and using these average measurements to create a single volumetric image of the fluidized bed at the different stable air flow rates.

This image is comprised of three-dimensional pixels, or voxels, the values of which correspond

to the average solids volume fraction within the 3D space represented by the individual voxels. The voxel values are represented visually as colors in the image, which means that the fluidized bed is viewed as a heat map of colors, exhibiting regions of higher and lower solid volume fractions. Different cross sections and lines of this image can be further analyzed and plotted. These plots were used to analyze the average solids fraction along the center axis and along the diameter of the column. Figures 5, 6, 8, and 9 show average radial and axial solids volume fraction in the fluidized beds.

Real-time images of bubbles in the fluidized beds were used to generate the third column of Tables 1 and 2. Figures 10, 11, and 12 show examples of ECVT real-time images of bubbles rising through the beds. For clarity, the image color gradients were scaled to show fully-packed solids as red and gas as blue.

The bubble images were also used to calculate average bubble velocity. This was done by measuring the amount of time (in seconds) it took a bubble to travel an axial distance of 2 inches (5.08 cm) within the sensing region. This process was done for several bubbles for each flow condition, in order to generate the fourth column of Tables 1 and 2.

Using all of the above ECVT analysis tools, it was seen that the Class A aluminum oxide particles fluidized more easily than the Class B sand particles. The Class A particle bed exhibited larger bubbles that flowed within an annular low-solids region at a higher velocity and more frequently than the bubbles produced in the Class B particle bed.

The Class B particle fluidized bed did not exhibit such an annular void region. Instead, bubbles expanded as they moved upward through the fluidized bed. These bubbles flowed in a less predictable way—some moved upward in the center of the column, some moved upward

along the side wall of the column. As the air flow rate was increased, the average bubble radius, velocity, and frequency increased.

The flow patterns observed utilizing ECVT correspond with the well-known fluidization tendencies of Geldart Class A and B particles. The Class A aluminum oxide bed fluidized easily and had a well-behaved flow with an annular low-solids region through which bubbles rose. The Class B sand bed required a higher air flow rate to reach fluidization and exhibited a more erratic, bubbly flow.

V. Conclusions

Electrical Capacitance Volume Tomography is a noninvasive, real-time imaging and measurement technique that can be used effectively for the online analysis of fluidized beds. This is beneficial for the close monitoring of gas-solid reactions and can be used to optimize the processes. The extensive analysis that can be done with Electrical Capacitance Volume Tomography make it the ideal technique for the imaging and control of fluidized beds.

VI. References

- [1] D. Kunii, O. Levenspiel, in *Fluidization Engineering, Second Edition*, Howard Brenner, ed., p. 77, Butterworth-Heinemann, a division of Reed Publishing, 1991.
- [2] W. Warsito, Q. Marashdeh, L.S. Fan, *Electrical Capacitance Volume Tomography*, IEEE Sensors Journal 7 (3-4) (Mar-Apr. 2007) 525-535.
- [3] Q. Marashdeh, *Validation of Electrical Capacitance Volume Tomography with Applications to Multi-Phase Flow System* [Masters of Science], The Ohio State University, Columbus, OH, 2009.
- [4] D.J. Holland, Q. Marashdeh, C.R. Muller, F. Wang, J.S. Dennis, L.S. Fan, et al., *Comparison of ECVT and MR Measurements of Voidage in a Gas-Fluidized Bed*, Industrial and Engineering Chemistry Research 48(1) (Jan. 7 2009) 172-181.

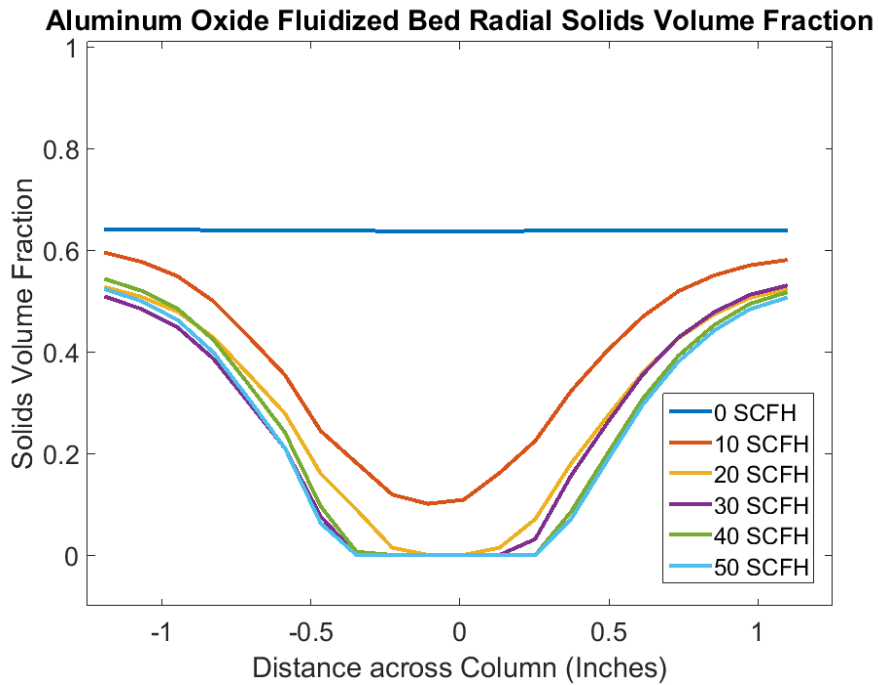
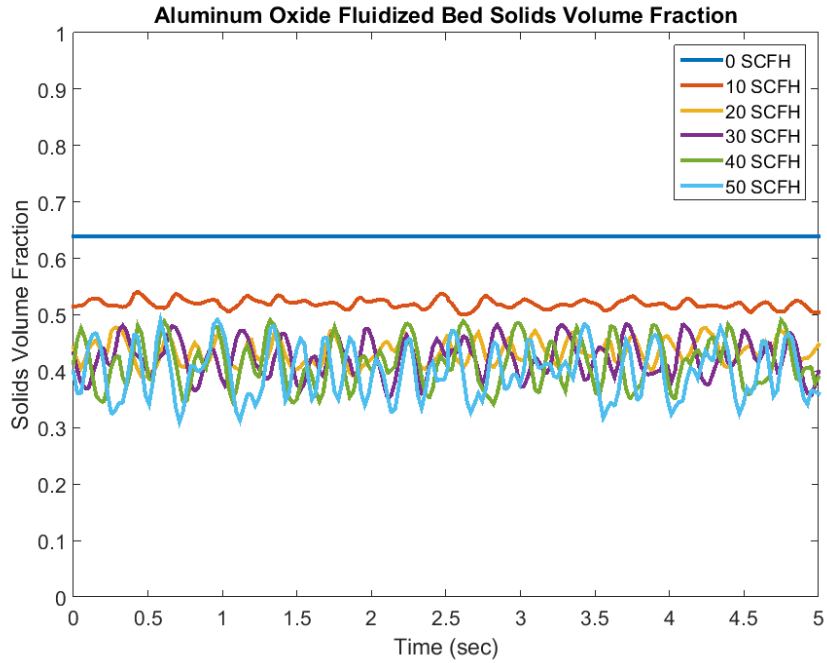


Figure 5: Aluminum Oxide Fluidized Bed Average Solids Volume Fraction across Column Diameter

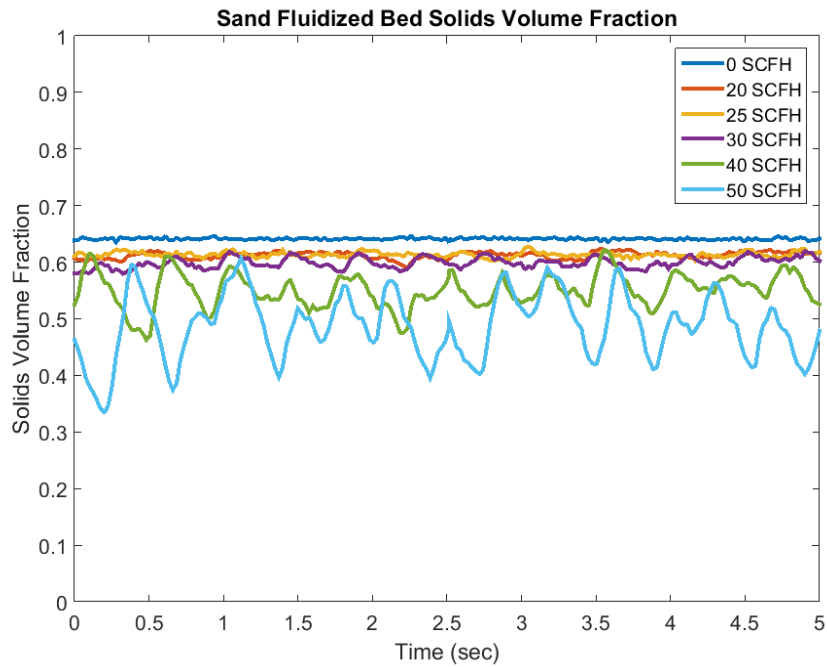
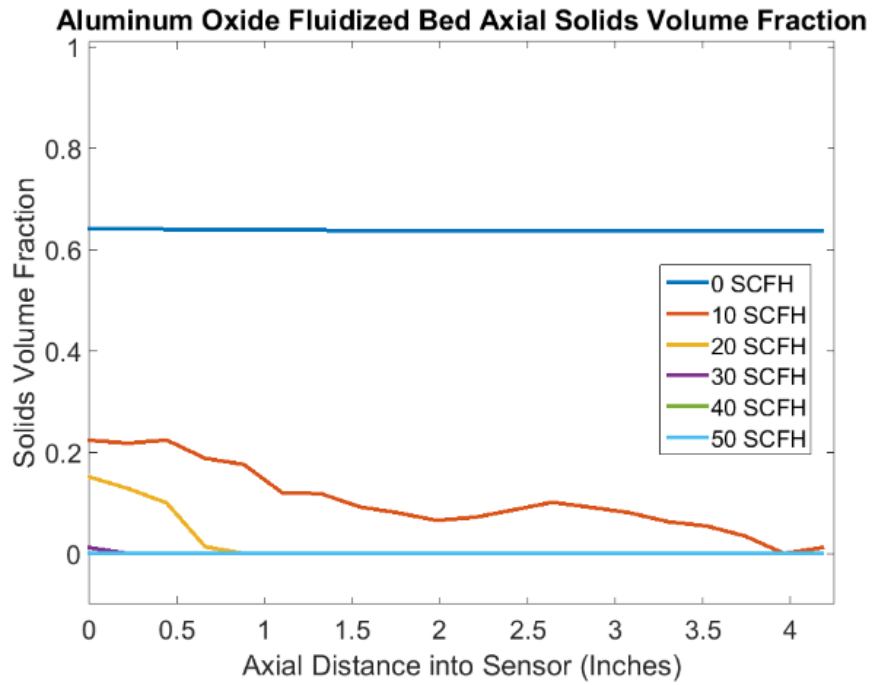


Figure 7: Sand Fluidized Bed Solids Volume Fraction over Time

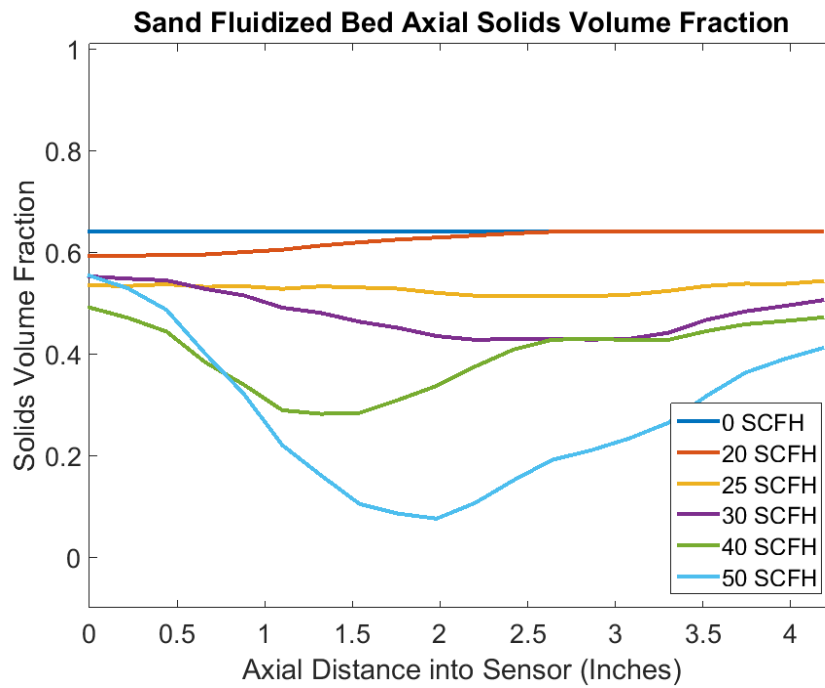
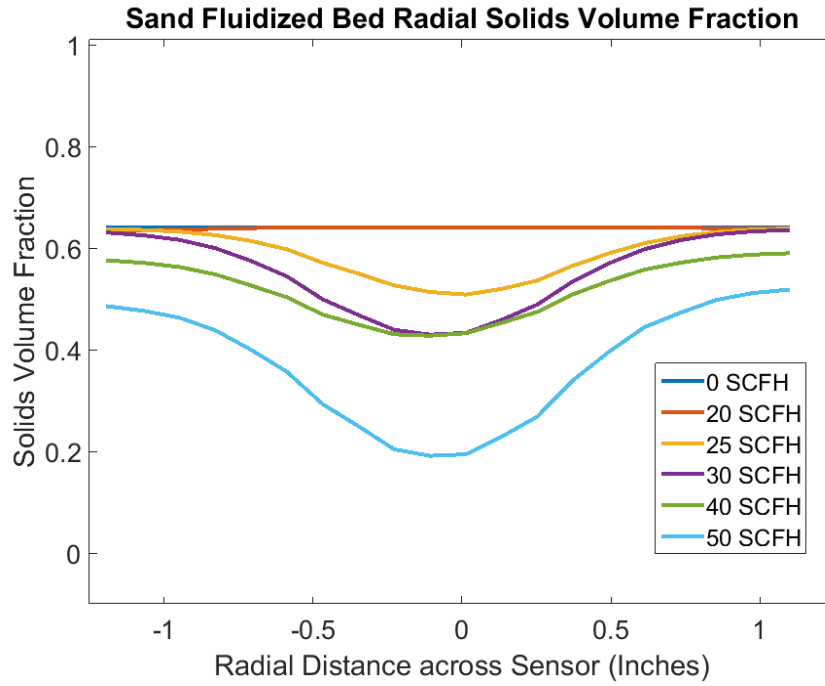


Figure 9: Sand Fluidized Bed Average Axial Solids Volume Fraction

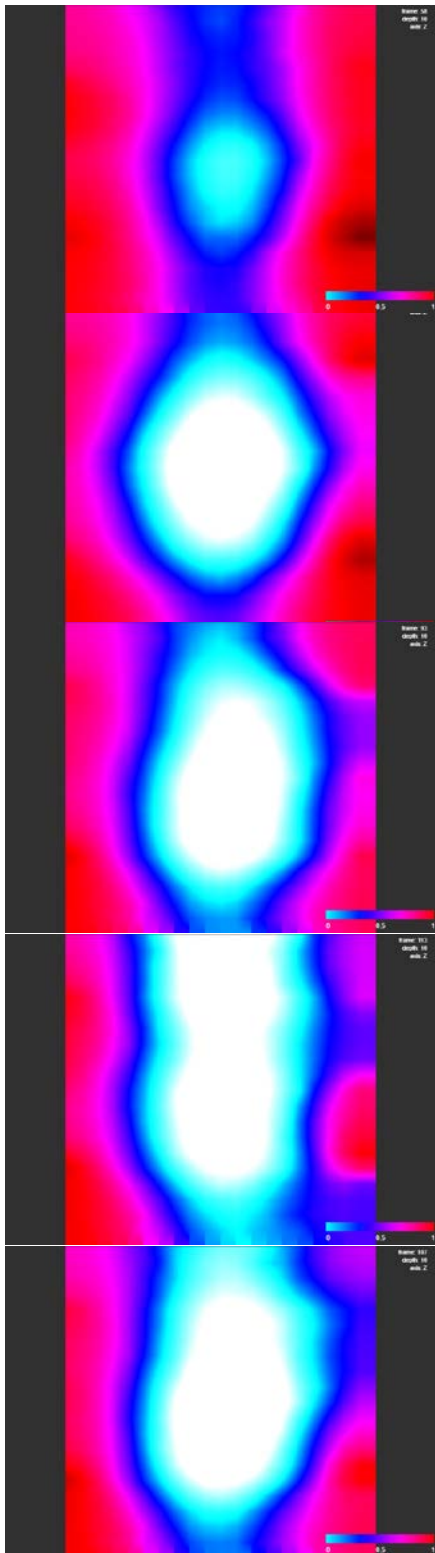


Figure 10: Axial cross section views of aluminum oxide fluidized bed at air flow rates of 10, 20, 30, 40, and 50 SCFH (blue = gas, red = solids)

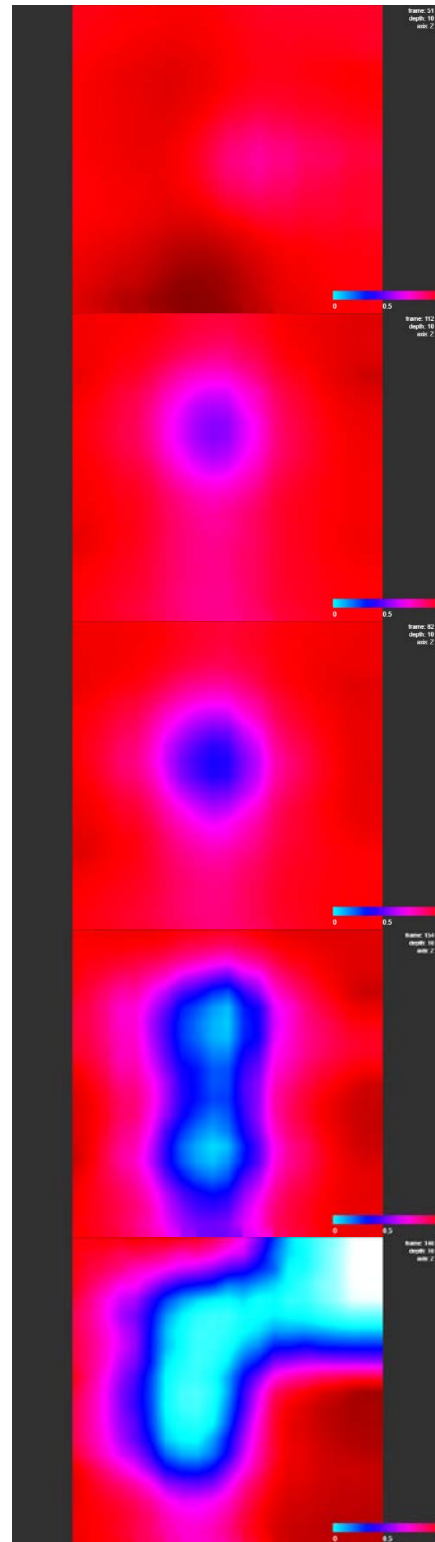


Figure 11: Axial cross section views of sand fluidized bed at air flow rates of 20, 25, 30, 40, and 50 SCFH (blue = gas, red = solids)

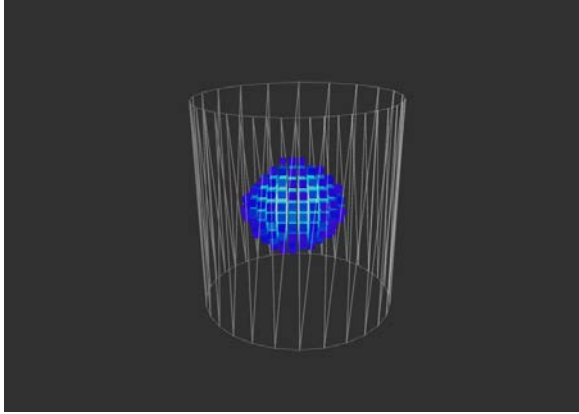


Figure 12: Three-dimensional image of bubble rising in sand fluidized bed (Air flow rate 50 SCFH)